Welding in the World (2020) 64:1671–1680
https://doi.org/10.1007/s40194-020-00939-7

RESEARCH PAPER

Investigation of residual stresses in polypropylene using hot plate welding

Andrea Wübbeke[1] · Volker Schöppner[1] · Bastian Geißler[2] · Michael Schmidt[2] · Arnaud Magnier[3] · Tao Wu[3] · Thomas Niendorf[3] · Fabian Jakob[4] · Hans-Peter Heim[4]

Received: 16 April 2019 / Accepted: 14 June 2020 / Published online: 5 August 2020

Abstract

During the cooling process of the molten material, residual stresses appear because the reduced volume of the cooled material cannot fully fill the space formerly occupied by the molten material. The morphology in and around the weld is formed by different factors depending on the material and process parameters. Different morphological structures relate to different mechanical properties. The process parameters and the welding results including morphology and residual stress are linked together. In this article, residual stresses and the mechanical properties of a hot-plate-welded polypropylene specimen with 0.1 wt.-% content of carbon black are investigated in relation to the morphology. Different measurement positions and joining displacements of parts to be joined result in different residual stress states and morphological structures. The higher the joining displacement, the higher the residual stress. Investigations of the morphology show a relation between the size of the alpha spherulites and the joining displacement. Diffractions patterns of wide-angle X-ray scattering (WAXS) are not able to resolve the beta phase of the specimen.

Keywords Hot plate welding · Morphology · Residual stress

1 Introduction

Polypropylene (PP) is widely used in polymer industry, and welding of PP is an important process. Due to the welding process, residual stresses and different morphological structures appear based on different process parameters. For welding of polymers, no research has been published which investigated the residual stresses, the mechanical properties of the weld and the morphology of the material at the same time. In this study, the influences of the process parameters on the mechanical properties of PP with carbon black content of 0.1 wt% are investigated. Mechanical properties are

Recommended for publication by Commission XVI - Polymer Joining and Adhesive Technology

✉ Andrea Wübbeke
andrea.wuebbeke@ktp.upb.de

Volker Schöppner
volker.schoeppner@ktp.upb.de

Bastian Geißler
b.geissler@blz.org

Michael Schmidt
info@blz.org

Arnaud Magnier
Arnaud.magnier@gadz.org

Tao Wu
wu@uni-kassel.de

Thomas Niendorf
niendorf@uni-kassel.de

Fabian Jakob
jakob@uni-kassel.de

Hans-Peter Heim
heim@uni-kassel.de

[1] Kunststofftechnik Paderborn, Paderborn University, Paderborn, Germany

[2] Bayerisches Laserzentrum, Erlangen, Germany

[3] Kassel University, Kassel, Germany

[4] Institut für Werkstofftechnik—Kunststofftechnik, Kassel University, Kassel, Germany

characterized by tensile test. Furthermore residual stresses in the weld are measured by the hole drilling method. Finally, the morphological structures of the different specimens are characterized by analysing the distribution of alpha spherulite size and diffraction patterns by WAXS.

2 Related work

In hot plate welding, two joining partners are pushed towards a hot tool and heated to melting by conduction. After a defined time, the heated tool is removed and the joining partners are brought into contact with a defined joining displacement or joining force.

There have been several investigations into hot plate welding. Potente developed a dimensionless approach for the process of hot plate welding [1]. Bonten [2] explains the theoretical background of the welding process itself. The optimized process parameters for hot plate welding such as welding temperature and geometrical definitions can be found in [3]. Concerning residual stresses, Schnieders [4] investigated the correlation between the welding process parameters and the development of stress cracking. The relation between mechanical properties of polyolefin (e.g. the full notch creep test) and welding parameters is discussed in [5].

However, more research is required concerning possible correlations between the morphology of the weld and its strength. The morphology of hot plate welded parts is shown in [6] where a defined morphological zone is divided into four zones. Here, a zone of deformed spherulites can be seen. These deformed spherulites are an indicator for good mechanical properties [7].

In order to analyse the inherent structure of polymers, especially for welded parts, an overview of different analysis strategies is given by [8]. Based on the literature, there are three different types of spherulite structures, which differ in their density and lattice structure [9, 10]: alpha, beta and gamma. The gamma form appears under special conditions (high pressure, low molecular weight and a high shear rate) [11, 12]. There are several methods of characterizing the morphology of PP. One well-established technique is the wide-angle X-ray scattering (WAXS). With this method, it is possible to distinguish between all three types of spherulite structures based on their intensity pattern [9]. The alpha and beta form can be distinguished by a polarization microscope in addition to the birefringence [12–15]. For a better differentiation, a lambda plate can be used to colour the beta form differently [16, 17]. Looking at research focusing on morphological analysis, for example in [15], the morphology upon hot plate welding was investigated. In that study, the morphology in the welded structure was characterized using Raman microscopy.

Mechanical properties of semi crystalline polymers depend on the molecular weight, the type of the spherulites, the crystallinity ratio and the size of the spherulites [12]. For instance, the beta structure is tougher than the alpha structure [10]. Also, impact energy measurements show higher values for the beta structure than for the alpha structure [18]. However, a higher content of beta spherulites in PP reduces the Young's modulus [12].

There are several methods of measuring the residual stresses in polymers, which can be classified as non-destructive, semi-destructive and destructive. Certainly, these methods can be further subdivided on the basis of the measurement principles to quantify the residual stress states. The most widely used non-destructive method is X-ray diffraction (XRD), but it is only applicable for crystalline materials. Optical methods such as photoelasticity analysis make use of the birefringence of transparent material to measure the difference between the two principal stresses [19]. The hole drilling method (HDM), as a widely used semi-destructive method, is capable of providing reliable results within the range of 10 to 800 μm from the specimen surface. However, this process is complex and time-consuming. The residual stress measurement through HDM in isotropic metallic materials was standardized in ASTM [20]. This method was then extended to allow for measuring residual stresses in plastic materials

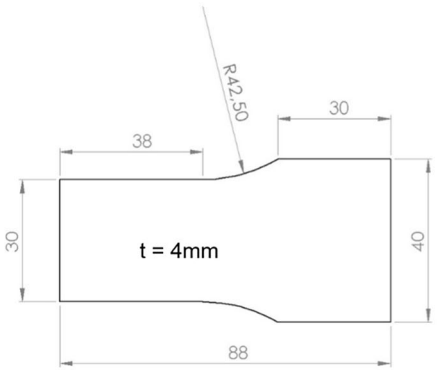

Fig. 1 Geometry of the joining part and welding parameters employed

Welding temperature = 220°C	
Joining displacement (s_j) [mm]	Ratio s_j/L_0 [n.a.]
0.361	0.3
0.6	0.5
0.9	0.75
1.14	0.95

s_j: Joining displacement
L_0: Melt layer
Melt layer = 1.2mm
Material: Polypropylene (PP) with 0.1 wt% of carbon black

accounting for the viscoelastic and thermal deformation occurring during and after drilling the material by [21, 22]. The reliability of residual stress measurements has been validated by mechanical bending tests using quenched polycarbonate samples with known residual stress profiles [22].

3 Experimental design

The specimens to be welded were produced by injection moulding. The geometry of a welding part is shown in Fig. 1 with a thickness of 4 mm. The welding temperature and the welding parameters are shown in the table and characterized by the right side of Fig. 1. To provide good mechanical properties of parts to be joined, the ratio of s_j/L_0 0.75 often is used [23]. The initial melt layer was measured according to [24].

The results of the tensile tests are given in Fig. 2. Five joined specimens were tested for each process parameter. The tensile strength is shown as a function of the joining displacement. The tensile strength increases as the joining displacement increases. For $s_j/L_0 > 0.75$, a plateau is observed.

In order to understand the mechanisms influencing the mechanical properties of the material, residual stresses are measured for two opposing process settings: samples with a ratio $s_j/L_0 = 0.3$ and $s_j/L_0 = 0.95$, both with a carbon black content of 0.1 wt%. The microstructure of the material will be shown respectively in chapter 5.

4 Residual stress

Applying the hole drilling method, a very small hole is drilled incrementally at the geometrical centre of a strain gauge rosette, which is glued to the surface of the part under consideration. The strains released upon drilling are measured. A schematic of a typical strain gauge and the used coordinate system for analysis are shown in Fig. 3, where the positive X direction is alongside the axis of strain gauge 1 and the negative Y direction alongside the axis of strain gauge 3.

After the layer-wise removal of material, a new equilibrium is established around the hole by releasing the residual stresses. The residual stress values are derived from the relaxed strains through

$$\varepsilon(\theta) = \frac{1+\nu}{E} a \frac{\sigma_x + \sigma_y}{2} + \frac{1}{E} b \frac{\sigma_x - \sigma_y}{2} cos(2\theta) + \frac{1}{E} b \cdot \tau_{xy} \cdot sin(2\theta) \quad (1)$$

where σ is stress, ε is strain, E is the Young's modulus and ν is the Poisson's ratio. In Eq. (1), the coefficients a and b can be analytically determined when a plate is drilled through, based on the Kirsch's law and the Hooke's law. For measuring a non-uniform residual stress state in an arbitrary material, the material needs to be drilled incrementally and Eq. (1) is required to be developed using the integral incremental formalism, i.e. applying the integral method, assuming that the stress is constant in each increment

$$\varepsilon_i(\theta) = \frac{1+\nu}{E} \cdot \sum_{j=1}^{i} a_{ij} \cdot \left(\frac{\sigma_x + \sigma_y}{2}\right)_j + \frac{1}{E} \cdot \sum_{j=1}^{i} b_{ij} \cdot \left[\left(\frac{\sigma_x - \sigma_y}{2}\right)_j \cdot cos(2\theta) + \tau_{xy_j} \cdot sin(2\theta)\right] 1 \le j \le i \quad (2)$$

Equation (2) can be written in a matrix form accounting for four increments

$$\begin{pmatrix} \varepsilon_1 \\ \varepsilon_2 \\ \varepsilon_3 \\ \varepsilon_4 \end{pmatrix}(\theta) = \frac{1+\nu}{2E} * \begin{bmatrix} a_{11} & 0 & 0 & 0 \\ a_{21} & a_{22} & 0 & 0 \\ a_{31} & a_{32} & a_{33} & 0 \\ a_{41} & a_{42} & a_{43} & a_{44} \end{bmatrix} * \begin{pmatrix} (\sigma_x+\sigma_y)_1 \\ (\sigma_x+\sigma_y)_2 \\ (\sigma_x+\sigma_y)_3 \\ (\sigma_x+\sigma_y)_4 \end{pmatrix} + \frac{1}{2E} * \begin{bmatrix} b_{11} & 0 & 0 & 0 \\ b_{21} & b_{22} & 0 & 0 \\ b_{31} & b_{32} & b_{33} & 0 \\ b_{41} & b_{42} & b_{43} & b_{44} \end{bmatrix} * \left(\begin{pmatrix} (\sigma_x-\sigma_y)_1 \\ (\sigma_x-\sigma_y)_2 \\ (\sigma_x-\sigma_y)_3 \\ (\sigma_x-\sigma_y)_4 \end{pmatrix} * \cos(2\theta) + 2 * \begin{pmatrix} \tau_{xy1} \\ \tau_{xy2} \\ \tau_{xy3} \\ \tau_{xy4} \end{pmatrix} * \sin(2\theta) \right) \quad (3)$$

In the incremental HDM, the strain ε_i measured after drilling the i_{th} increment is not only a function of the residual stresses σ_i present in the last drilled increment, but also a function of the residual stresses in all the previous increments. As mentioned before, the coefficients a_{ij} and b_{ij} only can be obtained based on an analytical solution in case of a through-thickness hole. For a blind hole and a non-uniform residual stress state analysis, respectively, calibration coefficients must be calculated by using finite element simulations, see [25] for more information.

In this work, the deformations during drilling were measured with strain gauges of the type Vishay EA-06-062RE-120. Concerning polypropylene samples, a primer needs to be used prior to bond the strain gauge on the surface for improving the adhesion between strain gauge and sample. The strain gauges were connected to an amplifier with a 0.5-V feed voltage. In doing so, the low voltage avoids generating too much Joule heat, which is crucial due to the low thermal conductivity of plastic materials. Nevertheless, the strain gauge signal is strongly unstable due to these heating effects, so that strain measurements were carried out only after 8 h following connecting the strain gauge to the amplifier. This allowed achieving thermal equilibrium, resulting in a satisfactory stable signal. The drilling process was done manually, with a drilling speed of about 20 rpm and a feed rate of about 0.03 mm/min. This low drilling speed avoids heating when drilling and, thus, no cooling system was used.

During drilling, the drilling tool pushes and shears the sample resulting in a viscoelastic deformation and that relaxes

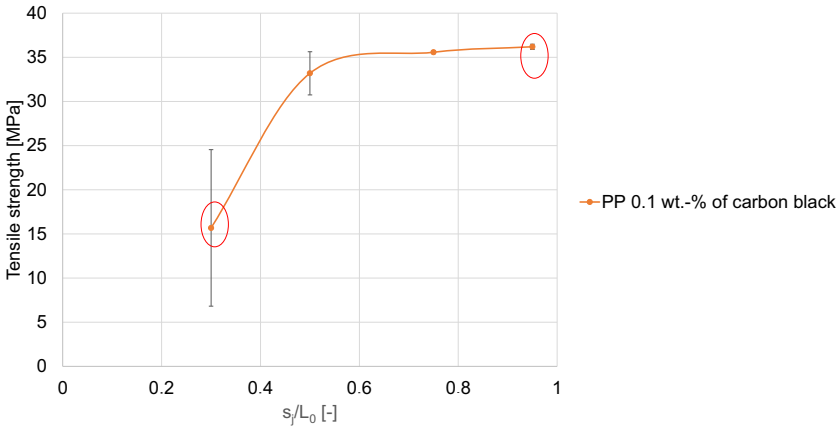

Fig. 2 Weld strengths due to different joining displacements

after drilling. Moreover, an additional elastic strain relaxation is caused by the removal of material and the relaxation of residual stresses. During each drilling step, the body heat of the operator and also other possible sources of heat affect the temperature at the strain gauge positions. Eventually, the accurate elastic strain relaxation accounting for the effects of the viscoelastic and thermal deformation occurring during and after drilling the sample can be determined with the aid of calibration coefficients, see [21] for more specific information.

After drilling, deformations are measured around the hole with strain gauges and are converted into residual stresses with the usage of calibration coefficients. This method was used in this work for the PP with 0.1 wt% of carbon black. Thereby, the strain gauge was placed directly on the weld, in direct vicinity of the weld bead and on the basic material. Further research is required to investigate material variations and positions. An increment of 0.1 mm was drilled in each case. After each drilling, a waiting period of 5 min was introduced until the next increment was drilled. Further increments are drilled without waiting for the given period of time; the measurement result will be falsified [26]. General details on the

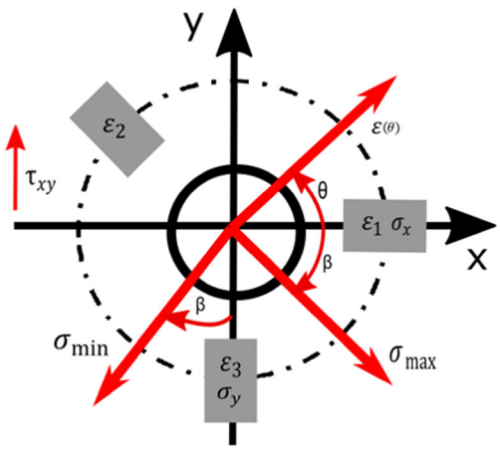

Fig. 3 Schematic representation of the strain gauge rosette applied and the coordinate system employed for the measurement of strain relaxation

coefficients and the principle of the hole drilling measurement can be found in ASTM [20].

To interpret the results of the measurement correctly, it is necessary to know which kind of qualitative distribution of stress can be expected. The results reported for the residual stress states of joined metals were taken from [27] as a basic reference for welded plastics for this purpose. Tensile residual stresses were seen in the weld seam, whereas the unwelded material as a basic reference for residual compressive stresses is characterized.

Measuring positions for determination of the residual stresses are shown in Fig. 4. The welded specimens were investigated by using different measuring positions. Measurements directly in the weld (by removing the weld bead) were performed for the joining displacements of 0.361 mm and 1.14 mm (as highlighted by the markings in Fig. 2). Reference material and a single spot near the weld bead were also investigated. The basic material was analysed in order to compare the residual stresses of welded and not welded material. The position near the weld bead was used to investigate whether a measurement directly in the weld or near the weld is possible in general.

The measurement of the residual stresses is separated into two measuring directions by the use of two figures. The y direction refers to the measurement alongside the weld (Fig. 5) and x direction transverse to the weld (Fig. 6). The residual stress measurement using the hole drilling method is relatively time-consuming and cost-intensive. Therefore, only one measurement was conducted per measuring point.

Figure 5 depicts the differences in residual stresses in relation to the depth of drilling for the y direction caused by the different joining displacements on one hand. The curves have the same shape except for near surface values (up to 0.1 mm). Values from 0 to 0.1 mm had to be excluded because of uncertainty in the measurement (for both directions). By looking at the maximum stresses, the joining displacement of 1.14 mm induced higher tensile residual stress than the joining displacement of 0.361. The higher the joining

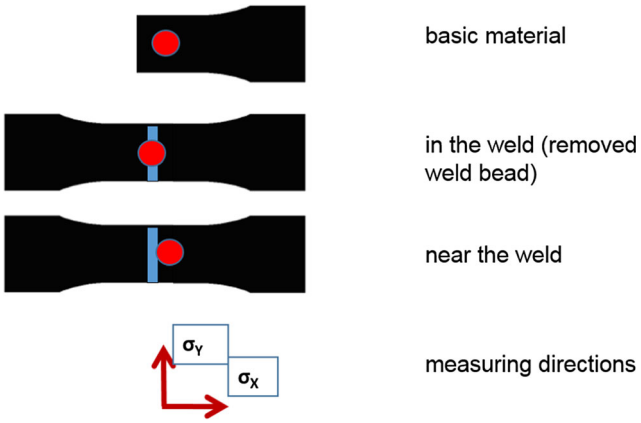

Fig. 4 Variation of measuring positions for the residual stress measurement

displacement is, the more squeeze flow occurs. In that way, the welding process induced more tensile residual stresses in case of higher joining displacements. At a surface distance of 0.3 mm, a higher joining displacement induced about 2 MPa more tensile residual stresses. On the other hand, the measurements near the weld and in the basic material, i.e. unaffected, reveal a different residual stress state. The position near the weld and in the basic material both shown compressive residual stresses. Residual stresses in the reference material are due to the processing of the sample. Compressive residual stresses near the surface of the material are characteristic for the injection moulding process [27]. Near the weld, the value of compressive residual stresses is lower than for the reference state, which may be due to the welding process, as it should induce tensile residual stresses directly near the weld seam.

A comparison of the different measuring positions near the weld and in the weld for the joining displacement of 1.14 shows a difference in their residual stress state direction as well. Near the weld, compressive stresses are found, whereas directly in the weld, tensile stress is observed. Results clearly indicate that a measurement directly in the weld generates acceptable values and is consequently an applicable methodology.

In contrast to the residual stress in the y direction shown in Fig. 5, Fig. 6 displays the results for the x direction. Comparing the two residual stress curves of $s_j = 1.14$ and $s_j = 0.361$, it becomes clear that they both are characterized by residual tensile stresses. Nominally, the maximum values of both curves are very similar. Maximal tensile residual stress of about 5 MPa in the direction x perpendicular to the weld is present at a depth of about 0.4 mm from the surface. Comparing these results of the residual stress measurement in x direction with the results of the tensile strength curves from Fig. 2, it becomes clear that the residual stresses determined are not the most important influencing factor with respect to the tensile strength. Both residual stress measurements reveal maximum values between 4 and 5 MPa. Assuming that the residual stress state would be a key influencing factor in terms of tensile strength, the residual stresses determined should have been significantly different in x direction (as the tensile strength values determined are significantly different).

At the two other measuring positions, the investigation of residual stresses near the weld and in the basic material shows a compression state as seen before in y direction. For this direction, the measuring position directly in the weld is most suitable for gaining robust measurement results.

5 Morphological analysis

For the morphological analysis, specimens were cut out of the welded parts and prepared by grinding and polishing for a permanganate etching with sulphuric acid, phosphoric acid and potassium permanganate. This method is used to remove

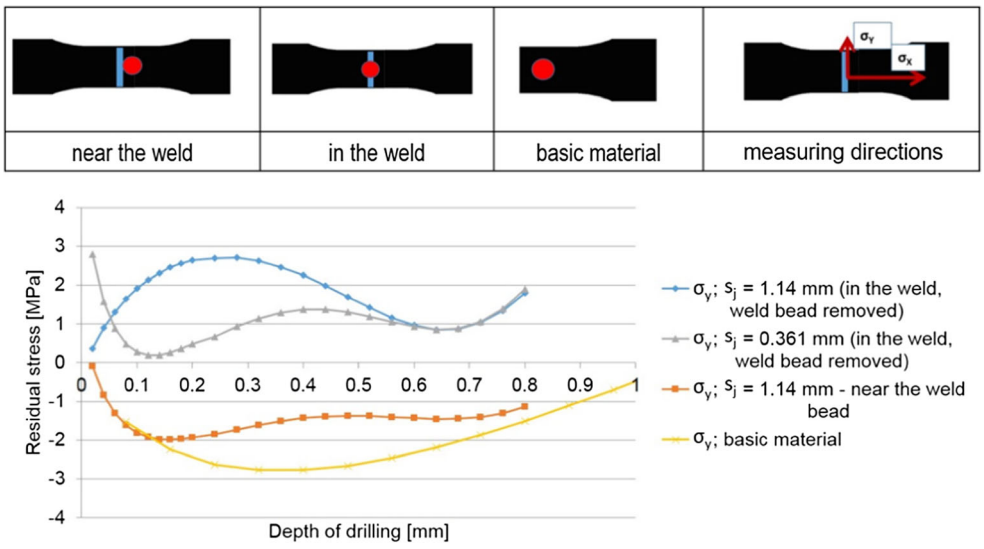

Fig. 5 Analysis of the residual stress of welded joints with different joining displacements for PP with 0.1 wt% carbon black, y direction

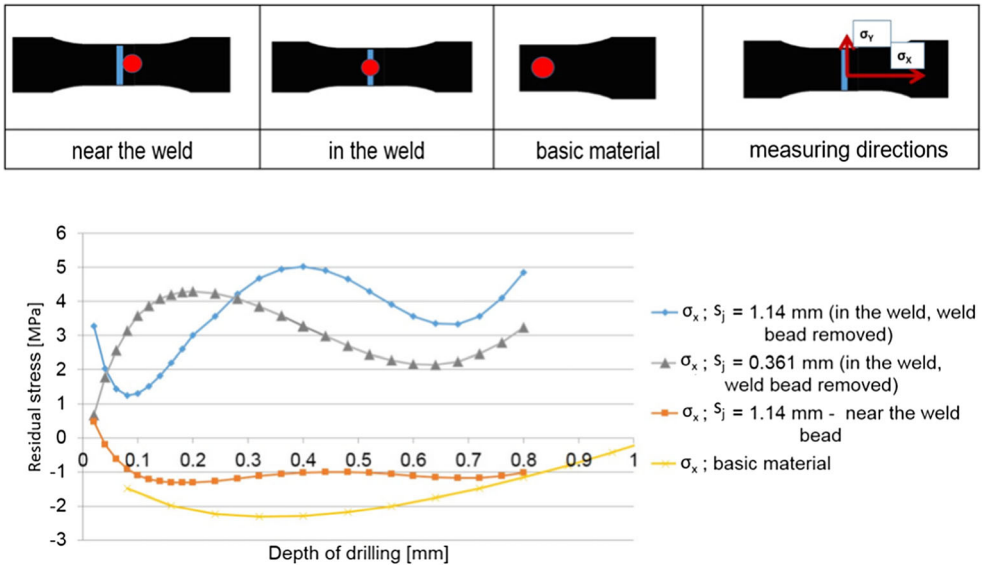

Fig. 6 Analysis of the residual stress of welded joints with different joining displacements for PP with 0.1 wt% carbon black, x direction

the amorphous areas of polyolefin polymers to make crystalline structures visible. A more detailed description of this etching method is given in [28].

The welded sections of the PP specimens coloured with carbon black show beta and alpha spherulites. Figure 7 shows an example of an etched weld of PP containing 0.1 wt% carbon black. The carbon black functions as a nucleation agent for beta spherulitic structures. As can be seen in Fig. 7, the appearance of a beta spherulite is dark, while the alpha spherulites seem to be brighter.

To analyse the morphology, the diameters of the alpha spherulites were measured with a confocal laser scanning microscope Olympus LEXT OLS3100. An investigation of the spherulite size in unwelded PP was done before by Way et al. [29]. They measured the spherulite size of moulded specimens and proved that small spherulites resulted in higher tensile strength than bigger spherulites. This clearly indicates that the diameter of the spherulites in welded specimens would have an impact on their mechanical properties. Hence, the size of the alpha spherulites of welded specimens in the middle of the weld seam was investigated for different joining displacements. The microscopic analysis reveals a correlation between the size of the alpha structure and the welding parameters. The higher the joining displacement is, the smaller the size of the alpha spherulites, as shown in Fig. 8.

Further, the interface structure already provides for an initial estimate of the final tensile strength. Figure 9 shows microscopic pictures of the interfaces for different joining displacements. For

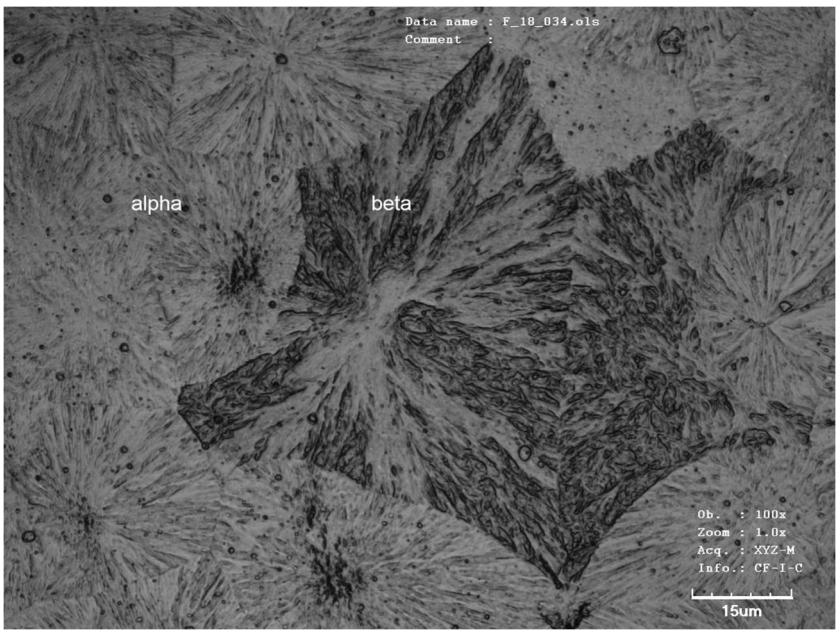

Fig. 7 Morphological analysis of the weld with beta and alpha spherulites

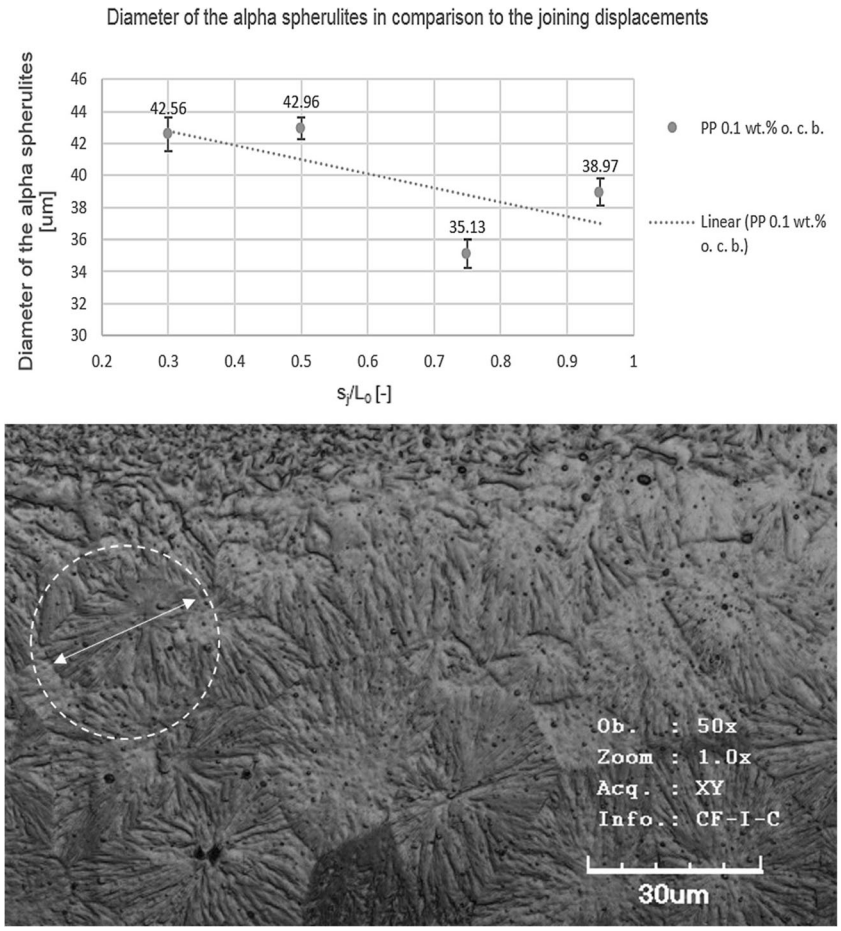

Fig. 8 Morphological analysis of the weld with alpha spherulites

the welding displacements of 0.361 mm and 0.6 mm, no flow lines can be found, while for larger displacements of 0.9 mm and 1.14 mm, significant flow lines arise.

Based on the guideline [23], a ratio of 0.75 for hot plate welding is optimal. The data in literature indicate that literature show that flow lines result in good mechanical properties (for vibration welding) [30]. This further indicates that the appearance of flow lines is able to reveal the difference between specimens with good and poor mechanical properties (for tensile strength) in terms of the hot plate welding process.

The flow lines, shown in Fig. 10, are related to deformed spherulites in the basic material. This content of deformed spherulites was also found in [30] for vibration welding and was shown to result in good mechanical properties. In [31], the flow lines are also found in a hot-plate-welded specimen. That investigation did not include different joining parameters, and only reported on the general appearance of these features.

The analysis by WAXS has been conducted for all welds. A bruker WAXS diffractometer in reflection mode in bragg-brentano configuration using Cu K (alpha) radiation as light source. The samples were rotated during the measurement. In every weld, the characteristic alpha pattern was found as seen in Fig. 11. The beta phase, which should be visible by a characteristic peak at 8 degrees, is not resolved. The carbon black, used as a nucleating agent, was not effective enough to lead to beta structure fractions being high enough to be detected. For investigations of the weld, a better way to see details is to use a reflecting microscope requiring a time-consuming etching process.

6 Conclusions

There are various possibilities for measuring residual stresses. In present work, the hole drilling method is used. The use of the hole drilling method is a challenge for joined components that have an externally visible weld bead. There are two options for determination of stresses. On the one hand, it is possible to measure next to the weld seam. This has the consequence that the original stress state in the weld seam is not changed. The stress state next to the weld seam is changed due to the local removal of material. Afterwards, the released strains are recorded and evaluated. The second possibility of stress measurement is the measurement directly in the weld seam. For this procedure, the weld bead must be removed in advance. This preparation step causes a change in the stress state itself. However, it allows to measure directly in the weld seam. The variation of the measuring position was primarily considered to show that principally a measurement in the weld

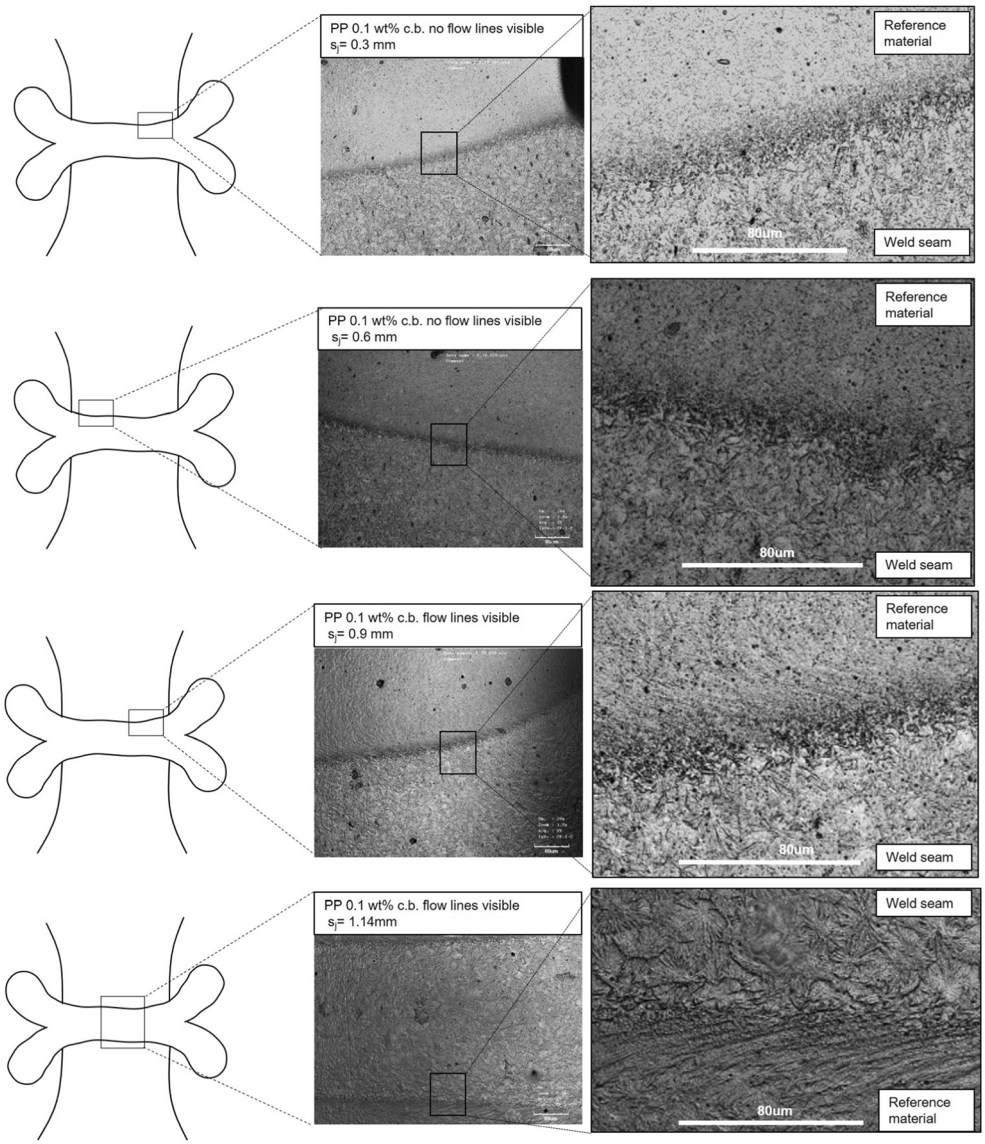

Fig. 9 Cross-sectional view of the weld area revealing flow lines appearing at joining displacements of 0.9 mm and 1.14 mm

seam itself is possible. The results obtained show that despite the removal of the weld bead, measurable tensile residual stresses are still present.

The experimentally determined residual stresses for the dimensionless joining displacements of 0.3 and 0.95 differ with respect to their maximum values. If one compares these maximum values with the results of the structural investigation focusing on the appearance of the alpha spherulite, the residual stresses increase with decreasing alpha spherulite dimensions. On the other hand, a larger alpha structure can give an indication of smaller residual stresses.

With reference to the results of the tensile tests, it has been shown that the residual stresses parallel to the loading direction. If the opposite would be true, the tensile direction probably would have no influence on the tensile strength. In this case, the tensile residual stresses would be very different, so that this trend finally would match the tensile characteristics.

The formation of the sheared zone can give an indication of the different residual stresses in x and y direction. However, the maximum values of both measurements differ by only about 1 MPa. It is therefore questionable, whether this structural feature can be used to predict the residual stress state correctly.

The decreasing spherulith radius, which is characteristic for the weld seam, indicates a trend to smaller alpha spherulithes. Since these values are also very similar, the characteristic of the deformed spherulites is only suitable for a rough estimation of the short-term tensile strength.

So far, no correlations have been established in literature between the alpha spherulith diameter of polypropylene and the residual stresses determined, neither in the weld seam nor for unjoined components. If the experimentally determined alpha spherulith radii are obtained with the maximum values of the residual stress analysis, a proportionality picture emerges. When maximum value of the residual stresses in

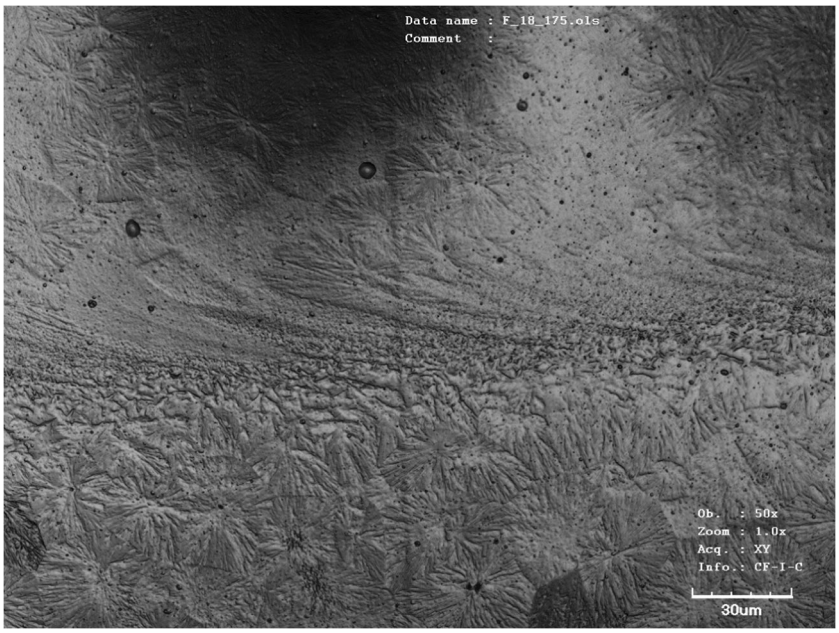

Fig. 10 Deformation of a spherulite as a starting point of flow lines

the weld increases for both directions, the alpha spherulite radius in the weld decreases. Since the values of the determined alpha spherulites are very similar, one can only speak of a tendency here as well.

7 Summary and outlook

In present work, hot-plate-welded specimens were analysed focusing on values of residual stress and yield strength as well as spherulite morphology. For specimens welded with higher joining displacement, higher tensile strength is revealed. The residual stress measurements showed that the joining displacement has a significant influence on the residual stress in the weld. Also, the location of the measurement has a significant effect on the results obtained.

In the welding zone, the structure of the specimens could be attributed to alpha and beta spherulites for polypropylene. A relation between the measured diameters of the alpha phase and the different joining displacements could be found. The appearance of flow lines is an indicator of joints with higher tensile strength.

In future work, the digital recognition of the patterns in the morphology could be used to gain more information about the regularity of the structure formed by the welding process. Also variation of measuring point could provide for more information on spherulite regularity. This may be mapped back to other mechanical properties such as impact energy and creep properties. Furthermore, the investigation of specimens with pure beta content is a topic for further research.

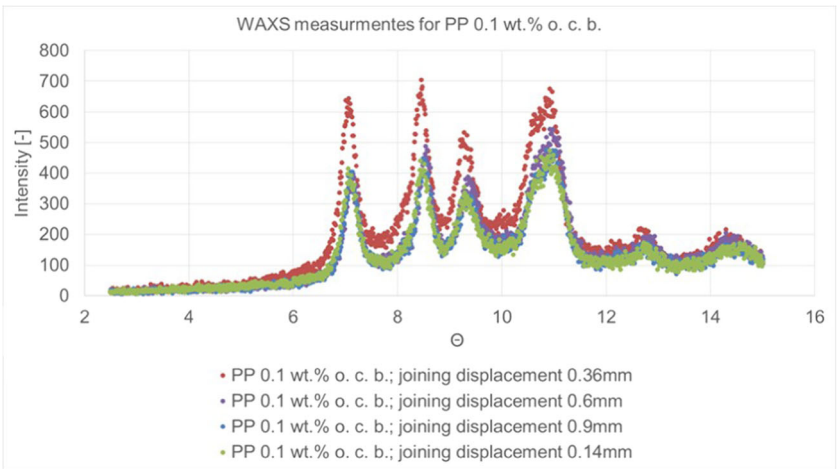

Fig. 11 WAXS measurement for PP 0.1 wt.% carbon black upon welding different joining displacements

Acknowledgements Open Access funding provided by Projekt DEAL. The authors thank the German Research Foundation (DFG) for funding this work (Schm2115/31-1,Scho551/20-1 and NI1327/19-1).

Abbreviations PP, polypropylene; WAXS, wide-angle X-ray scattering; s_j, joining displacement; L_0, initial melt layer; t_s, tensile stress; c_s, compression stress; σ_y, residual stress (y direction); σ_x, residual stress (x direction); HDM, hole drilling method

References

1. Joining plastics in production. Crampton, Sawston, Cambridge, UK, 1988 - ISBN 0853002029
2. Bonten C (1998) Beitrag zur Erklärung des Wirkmechanismus in Schweißverbindungen aus teilkristallinen Thermoplasten. Universität Gesamthochschule Essen, Dissertation
3. Optimierung der Schweißnahtfestigkeit von Heizelementstumpfschweißungen von Formteilen durch verbesserte Prozeßführung und Selbsteinstellung. DVS-Verl., Vol. 20, Düsseldorf, 1988 - ISBN 3871558796
4. Schnieders J (2004) Analyse der Fertigungs- und Prozeßeinflüsse auf die Spannungsrißbildung beim Fügen amorpher Thermoplaste mittels Heizelement. Universität Paderborn, Dissertation
5. Dietz R (2017) Strukturbezogene Betrachtung zum Zeitstandverhalten geschweißter Polyolefinhalbzeuge. Technische Universität Chemnitz
6. D. Grewell; A. Benatar; J. B. Park: Plastics and composites welding handbook. Hanser; Hanser Gardener, Munich, Cincinnati, 2003 - ISBN 3446195343
7. Handbook of plastics joining—a practical guide. Plastics Design Library, Norwich, NY, 1997 - ISBN 1884207170
8. A. Jungmeier; M. Vetter; E. Schmachtenberg: Charakterisierung der Struktur teilkristalliner Thermoplaste mittels Kleinwinkellichtstreuung. Practical Metallography, Vol. 46, Iss. 4, 2009, p. 173–193
9. T. Jones; J. M. Aizlewood; Beckett D. R.: Crystalline forms of isotactic polypropylene. Macromolecular Chemistry and Physics, Iss. 75, 1963, p. 1–236
10. Structure and morphology. Chapman & Hall, Vol. structure, blends and composites / ed. by J. Karger-Kocsis ; Vol. 1, London, 1. ed., 1995 - ISBN 978–0–412-58430-5
11. SPE/ANTEC 1996 Proceedings (Print version/ 3 volumes) K. Mezghani; P. J. Phillips: the morphology of the gamma form of isotactic polypropylene at 200 MPa, 1996
12. P. Tordjeman; C. Robert; G. Marin; P. Gerard: The effect of α, β crystalline structure on the mechanical properties of polypropylene. The European Physical Journal E, Vol. 4, Iss. 4, 2001, p. 459–465
13. W. Grellmann; S. Sabine: Kunststoffprüfung. Hanser, München, Wien, 2005 - ISBN 3–446–22086-0
14. K. Nakamura; S. Shimizu; S. Umemoto; A. Thierry; B. Lotz; N. Okui: Temperature dependence of crystal growth rate for α and β forms of isotactic polypropylene. Polymer Journal, Vol. 40, Iss. 9, 2008, p. 915–922
15. A. Sanoria; S. Damodaran; T. Schuster; R. Brüll: Investigating the morphological variations due to processing and thermomechanical treatment of poly(propylene) using Raman microscopy. Macromolecular Chemistry and Physics, Vol. 217, Iss. 9, 2016, p. 1037–1046
16. J. Varga; G. W. Ehrenstein; A. K. Schlarb: Vibration welding of alpha and beta isotactic polypropylenes—mechanical properties and structure. Express Polymer Letters, Vol. 2, Iss. 3, 2008, p. 148–156
17. Schuster T (2014) Dreidimensionale Charakterisierung von beta-nukleierten Polypropylen-Rohren mit Bildgebungsverfahren. Technischen Universität Darmstadt, Dissertation
18. S. C. Tjong; J. S. Shen; R. Li: Morphological behaviour and instrumented dart impact properties of β-crystalline-phase polypropylene. Polymer, Vol. 37, Iss. 12, 1996, p. 2309–2316
19. A. Adhikari; T. Bourgade; A. Asundi: Residual stress measurement for injection molded components. Theoretical and Applied Mechanics Letters, Vol. 6, Iss. 4, 2016, p. 152–156
20. Test method for determining residual stresses by the hole-drilling strain-gage method, 2013
21. Magnier A, Scholtes B, Niendorf T (2017) Analysis of residual stress profiles in plastic materials using the hole drilling method—influence factors and practical aspects. Polym Test 59:29–37
22. A. Magnier, B. Scholtes, and T. Niendorf, On the reliability of residual stress measurements in polycarbonate samples by the hole drilling method, Polymer Testing, 71, 329/334, 71, 2018
23. Heizelementschweißen von Formteilen aus thermoplastischen Kunststoffen in der Serienfertigung, 2010
24. H. Potente: Fügen von Kunststoffen - Grundlagen, Verfahren, Anwendung; mit 31 Tabellen. Hanser, München, Wien, 2004 - ISBN 978–3–446-22755-2
25. Magnier A, Zinn W, Scholtes B, Niendorf T (2018) Residual stress analysis on thin metal sheets using the incremental hole drilling method—fundamentals and validation. Exp Tech
26. Magnier A, Scholtes B, Niendorf T (2016) Analysis of residual stress profiles in plastic materials using the hole drilling method—influence factors and practical aspects. Polym Test 59:29–37
27. H. D. Tietz: Grundlagen der Eigenspannungen - Entstehung in Metallen, Hochpolymeren und silikatischen Werkstoffen, Meßtechnik und Bewertung. Springer-Verlag, Wien, 1982 - ISBN 3211958142
28. A. Breining; G. W. Ehrenstein; J. Varga: Ätzen von Kunststoffen. Eine Präparationstechnik für mikroskopische Untersuchungen, Vol. 39, Iss. 3, 1997, p. 81–85
29. J. L. Way; J. R. Atkinson; J. Nutting: The effect of spherulite size on the fracture morphology of polypropylene. Journal of Materials Science, Vol. 9, Iss. 2, 1974, p. 293–299
30. Giese M (1995) Fertigungs- und werkstofftechnische Betrachtungen zum Vibrationsschweißen von Polymerwerkstoffen. Universität Erlangen-Nürnberg
31. U. Egen: Gefügestruktur in Heizelementschweißnähten an Polypropylen-Rohren. Dt. Verl. für Schweißtechnik, Vol. 4, Düsseldorf, 1985 - ISBN 387155863 X
32. J. Mathar: Determination of initial stress by measuring the deformation around drilled holes. Transactions of the American Society of Mechanical Engineers, Vol. 56, Iss. 4, 1934
33. A. Nau; B. Scholtes; M. Rohleder; J. Nobre: Application of the hole drilling method for residual stress analyses in components made of polycarbonate. Zeitschrift Kunststofftechnik, Vol. 7, Iss. 3, 2011, p. 3–85